REMOTE SENS. ENVIRON. 30:77-87 (1989)

Mapping Surface Energy Balance Components by Combining Landsat Thematic Mapper and Ground-Based Meteorological Data

M. Susan Moran and Ray D. Jackson

U.S. Department of Agriculture, Agricultural Research Service, U.S. Water Conservation Laboratory, Phoenix

Lee H. Raymond

U.S. Geological Survey, Water Resources Division, Austin

Lloyd W. Gay

Department of Renewable Natural Resources, University of Arizona, Tucson

Philip N. Slater

Optical Sciences Center, University of Arizona, Tucson

Surface energy balance components were evaluated by combining satellite-based spectral data with on-site measurements of solar irradiance, air temperature, wind speed, and vapor pressure. Maps of latent heat flux density (λE) and net radiant flux density (R_n) were produced using Landsat Thematic Mapper (TM) data for three dates: 23 July 1985, 5 April 1986, and 24 June 1986. On each date, a Bowen-ratio apparatus, located in a vegetated field, was used to measure λE and R_n at a point within the field. Estimates of λE and R_n were also obtained using radiometers aboard an aircraft flown at 150 m above ground level. The TM-based estimates differed from the Bowen-ratio and aircraft-based estimates by less than 12% over mature fields of cotton, wheat, and alfalfa, where λE and R_n ranged from 400 to 700 Wm^{-2}.

Address correspondence to Ms. M. Susan Moran, U.S. Water Conservation Lab, 4331 E. Broadway Rd., Phoenix, AZ 85040.

Received 1 August 1989; revised 1 November 1989.

INTRODUCTION

The evaporation of water from soil and plant surfaces is a component of the surface energy balance that is of both theoretical and practical interest. It is an integral part of atmospheric circulation models, an important aspect of the global climate change issue, and constitutes a major part of the hydrologic cycle. In spite of its ubiquity, the relevance of evaporation in areal hydrologic applications, such as flood control and crop management, is limited by the difficulty involved in measuring it. Conventional ground-based methods for estimating evaporation, such as the Bowen ratio (Spittlehouse and Black, 1980), provide accurate measurements over a homogeneous area surrounding the instruments but the results are not applicable to large diverse areas. The only viable means of mapping the spatial distribution of evaporation on regional or local scales is remotely sensed spectral data from satellite-based sensors.

0034-4257/89/$0.00

On a regional scale, most methods for evaluating evaporation employ a numerical energy balance model in conjunction with satellite-based spectral data and meteorological data extrapolated from the nearest U.S. Weather Service meteorological station. Evaporation is generally estimated by using thermal infrared data acquired by satellite-based sensors and conventional ground-based meteorological data as inputs to a one-dimensional boundary layer model (Carlson and Boland, 1978; Carlson et al., 1981; Taconet et al., 1986; Soer, 1980). Gurney and Hall (1983) presented a method in which remotely sensed measurements of surface albedo, in addition to surface temperature and meteorological data, were used to calibrate an energy balance model and estimate daily evaporation. A variation on the modeling approach was presented in the Tellus project, where simulated day and night temperatures were compared with surface temperatures obtained from the satellite to determine thermal inertia and daily evaporation (Dejace et al., 1979; Rosema et al., 1978). Price (1980; 1982) proposed an analytical approach in which satellite-based measurements of surface temperature and reflectance were combined with meteorological data to estimate daily evaporation rates using the energy balance equation. Price corrected his estimates for small-scale micrometeorological effects by use of a numerical model.

Regional scale methods must necessarily rely on meteorological data from existing weather stations, which are generally located at nearby airports or government offices. These data are extrapolated in space and interpolated in time to correspond to the location and moment of the satellite overpass. At a local scale, such as an individual farming community or watershed, it is feasible to monitor meteorological conditions at the site during the time of satellite overpass. Thus, most local scale methods rely on site-specific measurements of aerodynamic and atmospheric conditions and apply only to an area over which the ground-based measurements can be extrapolated.

Jackson (1985) proposed that, on a local scale, the surface-dependent components of the energy balance (reflected radiation and surface temperature) could be evaluated remotely and combined with meteorological components (solar and sky radiation, air temperature, wind speed, and vapor pressure) to evaluate the energy balance over agricultural areas. This technique was successfully applied to data obtained using ground-based radiometers by Reginato et al. (1985) and aircraft-based radiometers by Jackson et al. (1987). The values obtained from aircraft-based sensors were compared with results from a Bowen-ratio apparatus in fields of cotton, wheat, and alfalfa on 5 days during a 1-year period. The aircraft-based and Bowen-ratio estimates of evaporation differed by less than 12% at the location of the Bowen-ratio instruments. At other locations, the aircraft-based technique detected substantial differences in evaporation resulting from differences in irrigation and crop density. This experiment emphasized the importance of evaluating the spatial distribution of evaporation.

This report describes an experiment in which data from satellite-based radiometers and ground-based meteorological instruments were combined to produce local maps of evaporation and net radiant flux density using the technique described by Jackson (1985). Landsat Thematic Mapper (TM) data were used to evaluate reflected radiation and surface temperatures, and ground-based meteorological instruments were used to measure solar and sky irradiance, air temperature, wind speed, and vapor pressure. The satellite-based estimates of evaporation were compared with results from the Bowen-ratio and aircraft-based methods. Accuracy assessment was limited to transects centered within large, uniform fields.

EVALUATION OF ENERGY BALANCE USING THE REMOTE METHOD

The procedure for estimating energy balance components from remote sensors and ground-based meteorological instruments has been described previously by Reginato et al. (1985), Jackson et al. (1987), and Jackson (1988). It is based on the evaluation of the energy balance equation, i.e.,

$$\lambda E = R_n - G - H, \tag{1}$$

where λE is the latent heat flux density [a product of the heat of vaporization λ ($J kg^{-1}$) and the rate of evaporation E ($kg s^{-1} m^{-2}$)], R_n is the net radiant flux density, G is soil heat flux density, and H is sensible heat flux density. Equation (1) is a one-dimensional form of the energy balance equa-

tion and it neglects the horizontal advective flow of heat and water vapor. All terms in Eq. (1) are in units of $W m^{-2}$ and values of λE, G, and H are positive when direction away from the surface.

Net Radiant Flux Density

Net radiant flux density (R_n) is the sum of incoming and outgoing radiant flux densities, i.e.,

$$R_n = R_{S\downarrow} - R_{S\uparrow} + R_{L\downarrow} - R_{L\uparrow}, \qquad (2)$$

where the subscripts S and L signify solar (shortwave) radiation (0.15–4 μm) and longwave radiation (> 4 μm), respectively. The arrows indicate the flux direction ($\downarrow$ = incoming, $\uparrow$ = outgoing). Jackson et al. (1985) proposed that the incoming terms ($R_{S\downarrow}$ and $R_{L\downarrow}$) be measured with traditional ground-based instruments and the data extrapolated radially for some distance from the point of measurement. Thus, incoming solar radiant flux density $R_{S\downarrow}$ can be measured with a calibrated pyranometer sensitive to radiation over most of the solar spectrum and incoming longwave radiant flux density $R_{L\downarrow}$ can be estimated from ground-based measurements of air temperature and vapor pressure using the relation

$$R_{L\downarrow} = \epsilon_a \sigma T_a^4, \qquad (3)$$

where $\epsilon_a = 1.24(e_0/T_a)^{1/7}$ (Brutsaert, 1975), σ = the Stefan–Boltzmann constant ($W m^{-2} K^{-4}$), T_a = air temperature (K), and e_0 = vapor pressure (mb).

The outgoing terms ($R_{S\uparrow}$ and $R_{L\uparrow}$) can be obtained from data collected with down-looking multispectral sensors. Jackson (1984) described a method by which the total reflected solar radiant flux density $R_{S\uparrow}$ (0.15–4 μm) was estimated from the radiance measured using a multispectral radiometer. The outgoing longwave radiant flux density $R_{L\uparrow}$ can be obtained from the remotely measured surface temperature,

$$R_{L\uparrow} = \epsilon_s \sigma T_s^4, \qquad (4)$$

where ϵ_s = surface emissivity and T_s = surface temperature (K) measured by a thermal radiometer. The value of ϵ_s can be determined for the surface of interest using a technique described by Taylor (1979).

Table 1. Spectral Bands of the Landsat Thematic Mapper Covering the Visible and Infrared (IR) Spectrum, Where δ Is the Nominal Spectral Response and IFOV Is the Instantaneous Field of View.

	Landsat TM		
Spectrum Label	*Band*	*δ (μm)*	*IFOV (m)*
Blue	TM1	0.45–0.52	30
Green	TM2	0.53–0.61	30
Red	TM3	0.62–0.69	30
Near IR	TM4	0.78–0.90	30
Mid IR	TM5	1.57–1.78	30
Mid IR	TM7	2.10–2.35	30
Thermal IR	TM6	10.42–11.66	120

Instantaneous λE

Calculation of λE depends upon the evaluation of R_n, G, and H [Eq. (1)]. The G term is traditionally measured with sensors buried just beneath the soil surface. G is dependent on surface vegetation cover and, therefore, a ground-based measurement should not be extrapolated spatially. A remote measurement of G is not possible, but a relation between G/R_n and spectral data in the red and near-infrared (NIR) wavebands (Table 1) can be determined for the time of overpass (Clawson[1]). The relation is

$$G/R_n = 0.583e^{-2.13\mathrm{ND}}, \qquad (5)$$

where ND is the normalized difference [(NIR − red)/(NIR + red)], a spectral index that estimates the amount of vegetation present.

The sensible heat flux density can be expressed as

$$H = \rho c_p (T_s - T_a)/r_a, \qquad (6)$$

where ρc_p is the volumetric heat capacity ($J m^{-3} C^{-1}$) and r_a is a stability-corrected aerodynamic resistance ($s m^{-1}$) as given by

$$r_a = \left\{\ln[(z - d + z_0)/z_0]/k\right\}^2 \times (1 + 15\mathrm{Ri})(1 + 5\mathrm{Ri})^{1/2}/U, \qquad (7)$$

(adapted from Mahrt and Ek, 1984) for the stable case [$(T_s - T_a) < 0$], and

$$r_a = \left\{\ln[(z - d + z_0)/z_0]/k\right\}^2 \times \left\{1 - 15\mathrm{Ri}/\left[1 + C(-\mathrm{Ri})^{1/2}\right]\right\}^{-1}/U, \qquad (8)$$

[1]Personal communication, K. L. Clawson, formerly at the U.S. Water Conservation Laboratory, Phoenix, AZ, now with NOAA, Idaho Falls, ID.

for the unstable case $[(T_s - T_a) > 0]$. In Eqs. (7) and (8), Ri is the Richardson number $[\mathrm{Ri} = g(T_a - T_s)(z - d)/T_a U^2]$, g the acceleration due to gravity ($\mathrm{m\,s^{-2}}$), U the wind speed ($\mathrm{m\,s^{-1}}$), z the height (m) above the surface at which the wind speed and air temperature are measured, d the displacement height (m), z_0 the roughness length (m), k von Karman's constant (0.4), and $C = 75k^2[(z - d + z_0)/z_0]^{1/2}/\{\ln[(z - d + z_0)/z_0]\}^2$. Equations (7) and (8) are used to characterize one-dimensional heat flow and are probably valid for use within large homogeneous regions with fully developed internal boundary layers.

IMAGE PROCESSING

The Landsat TM sensor covers a range of wavelengths (Table 1) similar to the hand-held and airborne radiometers used in previous experiments. However, use of TM data in the remote energy balance model posed several new problems, in particular, 1) atmospheric correction of data obtained by visible, near-infrared, and thermal sensors and 2) compensation for coarse spatial resolution of the TM thermal band (TM6) relative to the resolution of the reflective bands.

Atmospheric Correction

The Landsat TM digital counts (DCs) obtained from the computer compatible tape (CCT) in TM1–TM4 were converted from radiometrically corrected values to the original DC values using the radiometric correction factors supplied with the CCT in the radiometric look-up table (RLUT). Absolute radiance values, uncorrected for atmospheric effects, were calculated from the original DCs by use of TM sensor calibration coefficients. Atmospheric effects on the days of overpasses were characterized by Langley plot measurements to determine Rayleigh, Mie, and ozone optical depths (Slater et al., 1987). These values were used as inputs to a radiative transfer model to compute surface reflectance and radiance corrected for atmospheric effects. Holm et al. (1989) described the atmospheric correction procedure in detail.

The process of converting TM thermal data to values of surface temperature requires correction for atmospheric water vapor content. Vertical profiles of atmospheric water vapor content are generally acquired by radiosonde measurements at the time of overpass. Since radiosonde data were not available on these dates and since our primary objective was to demonstrate the feasibility of producing images of energy balance components, we chose to circumvent this problem by extracting transects of the TM6 digital data (DC) along the center of 12 fields from each scene and registering each transect to the aircraft-based thermal data (T_s) collected at the time of overpass. Linear regression equations were computed for each date from these data sets, where $T_s = a(\mathrm{DC}) + b$ (see example in Fig. 1). Correlation coefficients (R^2) for all three dates were greater than 0.90.

TM6 Spatial Enhancement

A method to enhance the spatial resolution of the 120 m thermal data was developed in order to compensate for differences in the spatial resolution of the TM bands (Moran, 1990). The method is applicable to areas characterized by discrete fields having relatively uniform cover within fields. The key to this method lies in the fact that the Landsat-TM reflective bands are spatially registered with TM6 and are acquired at a spatial resolution 16 times that of TM6 (30 m). The enhancement method is a three step process: 1) field boundaries are defined based on common values in the high resolution reflective bands; 2) within each designated field, the statistical mode of the original thermal data is computed; and 3) a new thermal image is created based on the modes of the original thermal data. This technique is based on the assumption that the mode of the data, that is, the value that occurs most frequently in a given field, is representative of the actual thermal emittance from that field and that values obtained on field boundaries will be contaminated by a variety of bordering cover types and thus will vary much more than the values in the field center.

EXPERIMENTAL SITE AND PROCEDURE

The experimental site was the 770 ha University of Arizona Maricopa Agricultural Center (MAC), about 48 km south of Phoenix, Arizona. From June 1985 to June 1986, atmospheric measurements, aircraft-mounted radiometer measurements and meteorological measurements were made on each

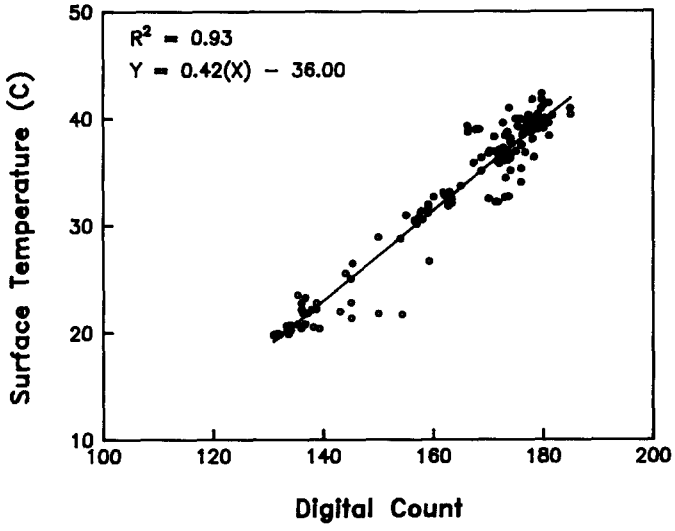

Figure 1. Regression of Thematic Mapper Band 6 (TM6) digital counts with aircraft-based measurements of surface temperature over 12 fields at the time of Landsat Thematic Mapper overpass, 24 June 1986.

day of the Landsat-5 overpass, weather and equipment permitting. Data reported here are limited to the dates when TM data were acquired and Bowen-ratio data were collected and to fields in which the Bowen-ratio equipment was located. These dates were 23 July 1985, 5 April 1986, and 24 June 1986. The Bowen-ratio equipment was located in a cotton field (0.27×1.6 km) on 23 July 1985, a wheat field (0.27×1.6 km) on 5 April 1986, and an alfalfa field (0.14×0.8 km) on 24 June 1986.

The equipment mounted in the aircraft included a four-band multispectral radiometer, a single band thermal infrared thermometer, and a video camera. In flight, the instruments viewed normal to the surface with a nominal 15° field of view. At an altitude of about 150 m above ground level (AGL), a circular area of about 40 m diameter was sampled on the ground. A data logger recorded the output from the five channels and the time (to 0.0001 h) at 2-s intervals. A character generator on the video system recorded the elapsed time on each frame. The video time and data logger time were used to identify the video frame corresponding to a particular sample.

A portable micrometeorological station, located in the same field as the Bowen-ratio equipment, recorded incoming solar radiation, wet and dry bulb air temperature, and wind speed (at 1.5 m) at 6-s intervals. Fluctuations of the 6-s wind speed values were reduced by smoothing the data with a 30-point (3-min) running average. These measurements provided data for the calculation of $R_{S\downarrow}$, $R_{L\downarrow}$, and r_a, of Eqs. (2), (7), and (8).

The Bowen-ratio apparatus consisted of a psychrometer exchange mast, a net radiometer, a soil heat flux plate, anemometer, and a data acquisition and processing system (Gay and Greenberg, 1985). The net radiometer and the anemometer were placed 2 m above the soil surface. The soil heat flux plate was buried about 1 cm below the soil surface. The psychrometer mast interchanged the sensors at 6-min intervals (to minimize instrument bias in the gradient measurements), allowing evaporation calculations to be made on 12-min averages.

Values of R_n and λE were calculated using estimates of radiance from the aircraft-based radiometer. The airborne radiometer data were converted to radiance values by use of calibration factors provided by the manufacturer. The radiances of the four bands were summed and used to estimate values of $R_{S\uparrow}$ [Eq. (2)]. The radiometric surface temperature, that is, the temperature measured with the airborne infrared radiometer (IRT), was used to calculate $R_{L\uparrow}$ [Eq. (3)]. To obtain the surface–air temperature difference $(T_s - T_a)$ for Eq. (6), the radiometric temperatures were corrected for surface emissivity by multiplication by $\epsilon_s^{-1/4}$. Values of ϵ_s were estimated to be 0.985 for cotton, 0.980 for alfalfa and wheat, and 0.940 for bare rough soil, based on field measurements using a technique described by Fuchs and Tanner (1966). Values of z_0 and d, for input to the calculation of

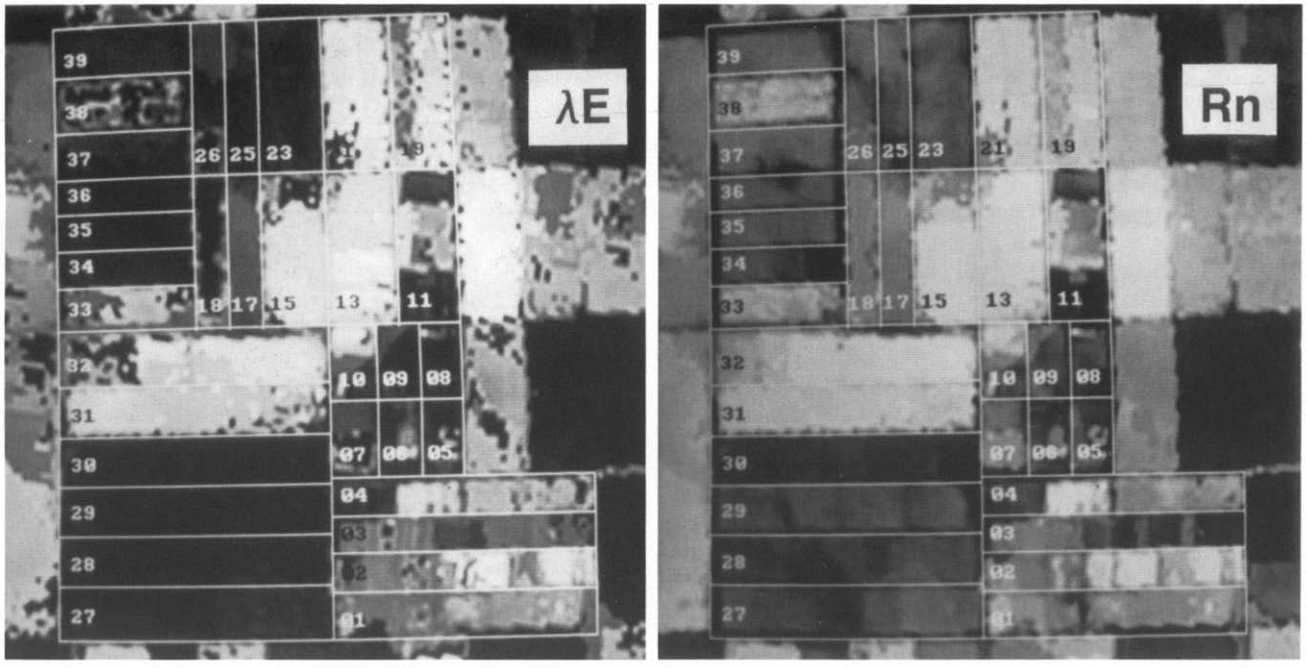

(a) (b)

Figure 2. Maps of instantaneous latent heat flux density (λE) and net radiant flux density (R_n) (24 June 1986) based on Landsat Thematic Mapper (TM) spectral data and ground-based meteorological data. Grey levels relate directly to the magnitude of flux density ($W m^{-2}$), where white designates the highest value and black the lowest. Over the ground surface covered by each map (approx. 20 km^2), values of R_n ranged from 240 to 640 $W m^{-2}$ and values of λE ranged from 0 to 1080 $W m^{-2}$. The images are overlain with the Maricopa Agricultural Center (MAC) field boundaries and numerical field designations.

r_a [Eqs. (7) and (8)], were estimated from field measurements of plant height (h), where $z_0 = 0.13h$ and $d = 0.63h$ (Monteith, 1973). The G term was estimated from R_n using the spectral data to calculate the fraction G/R_n [Eq. (5)].

The Landsat CCT-A digital counts were converted to radiance values as described previously and the radiances of the first four reflective bands were used to yield values of $R_{S\uparrow}$. The surface temperatures, measured by the TM6, were used to calculate $R_{L\uparrow}$ and $(T_s - T_a)$. Since ϵ_s, z_0, and d could not be estimated remotely using this data set, values were assigned to each TM image element (pixel) based on the value of ND. That is, threshold values of ND were determined to separate soil, alfalfa, wheat, and cotton and values of ϵ_s, z_0, and d (discussed in the previous paragraph) were assigned to areas encompassed by each cover type. Estimates of G were made using Eq. (5) with the TM-based images of R_n and ND, corrected for atmospheric effects. The accuracy of remote estimates of G were found to be adequate for this data set and this application by Jackson et al. (1987).

Daily totals of λE can be determined from instantaneous values using a method described by Jackson et al. (1983), assuming wind speed remained relatively constant over the day. The conversion of instantaneous values to daily totals was analyzed for this data set by Jackson et al. (1987) and will not be repeated here.

RESULTS AND DISCUSSION

Maps of instantaneous λE and R_n (24 June 1986) based on Landsat TM spectral data and ground-based meteorological data are presented in Figure 2. The maps are overlain with the MAC farm field boundaries and numerical field designations. Values of λE and R_n are directly related to the range of grey levels portrayed in the map, where light and dark areas indicate high and low flux densities respectively. The data presented in Figure 2 illus-

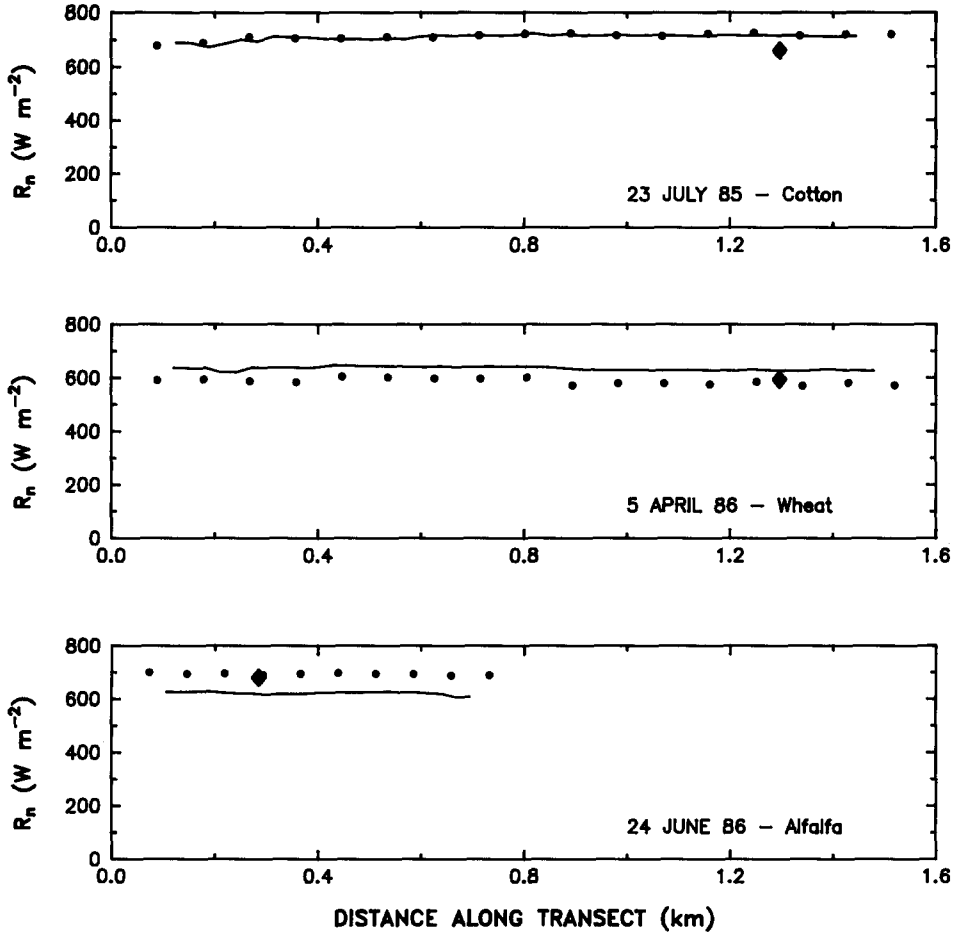

Figure 3. Values of net radiant flux density (R_n) based on Landsat Thematic Mapper (TM) data (—), aircraft-based data (●), and the ground-based net radiometer (◆) for fields of alfalfa, wheat and cotton. Data are plotted to simulate their approximate location along a transect through the center of the field.

Figure 4. Estimates of net radiant flux density (R_n) at the location of the Bowen-ratio apparatus in the cotton, wheat, and alfalfa fields on 23 July 1985, 5 April 1986, and 24 June 1986, respectively.

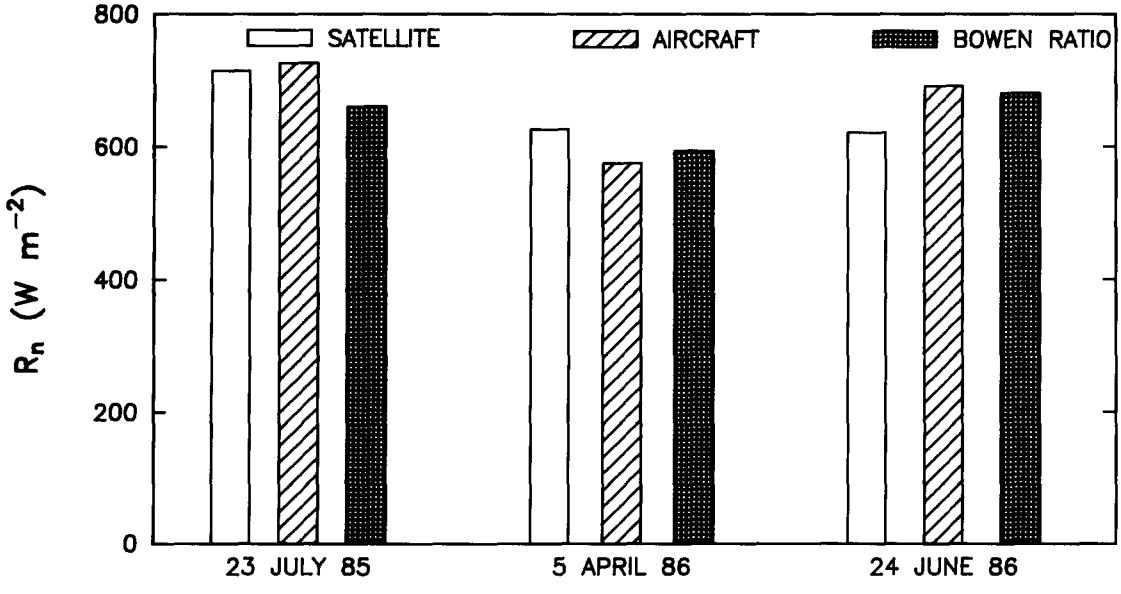

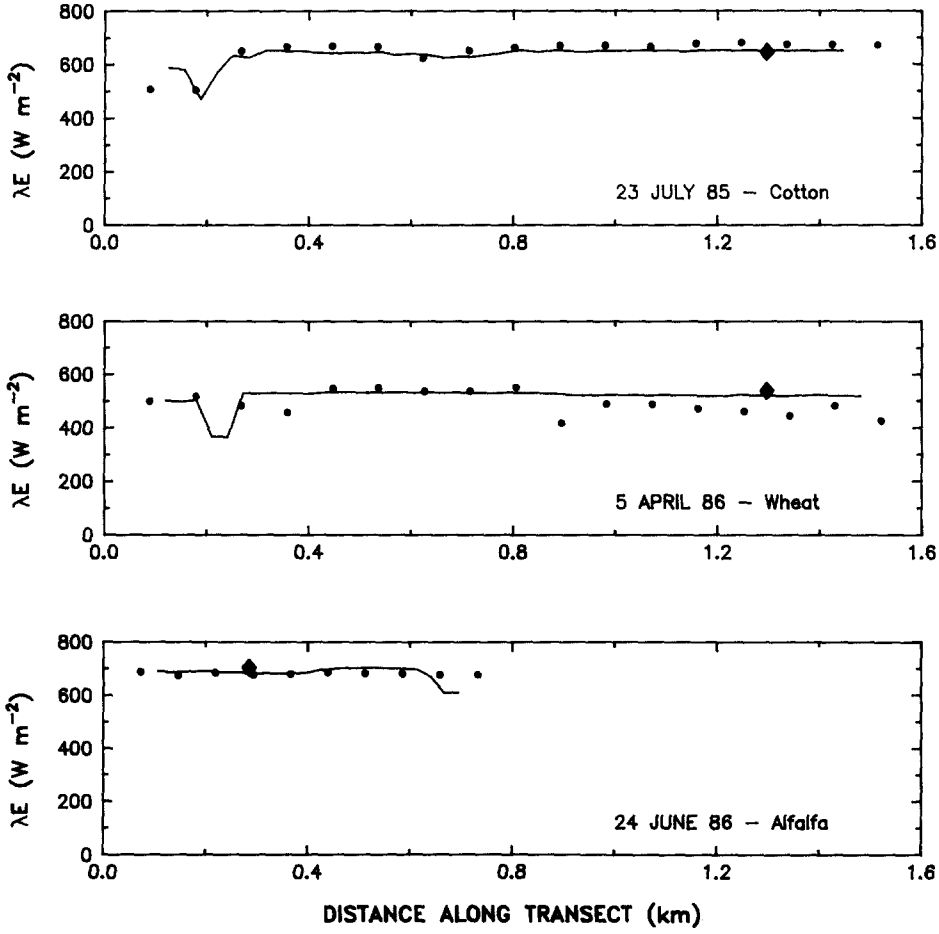

Figure 5. Values of latent heat flux density (λE) based on Landsat Thematic Mapper (TM) data (—), aircraft-based data (●), and the ground-based net radiometer (◆) for fields of alfalfa, wheat, and cotton.

Figure 6. Estimates of latent heat flux density (λE) at the location of the Bowen-ratio apparatus in the cotton, wheat, and alfalfa fields on 23 July 1985, 5 April 1986, and 24 June 1986.

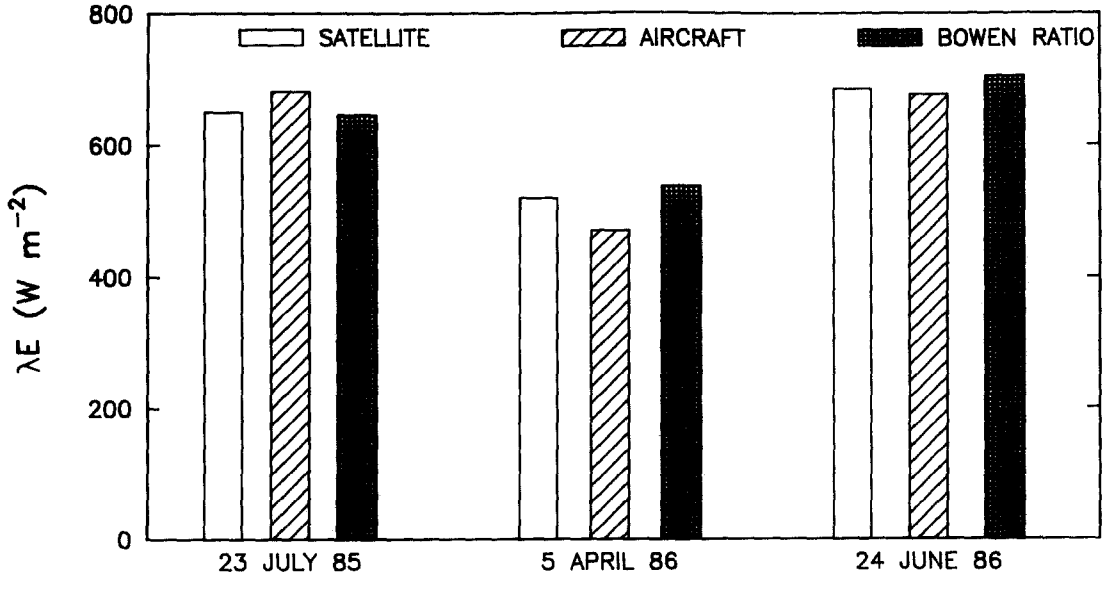

trate both the between- and within-field diversity of λE and R_n. Over the ground surface covered by each map (approx. 20 km^2), values of R_n ranged from 240 to 640 Wm^{-2}, values of λE ranged from 0 to 1080 Wm^{-2} and values of sensible heat flux density (H) were occasionally in excess of 400 Wm^{-2}.

The within-field variation is best illustrated by data in Field #32 (Fig. 2), a cotton field in which the west two-thirds of the field had been irrigated during the previous 24-h period and the east third had not been irrigated for more than 2 weeks. Estimates of R_n from the west end of the field differed from the east end by 12% and the difference in values of λE was greater than 50%.

Values of R_n calculated from Landsat TM data, aircraft-based data, and the ground-based net radiometer for fields of alfalfa, wheat, and cotton are shown in Figure 3. Data are plotted to simulate their approximate location along a transect through the center of the field. The TM overflights and the aircraft flights were made near 1030 MST on each day. The 12-min average of the ground-based net radiometer on the Bowen-ratio apparatus nearest the time of overpass was used for comparison.

Data presented in Figure 4 illustrate the concurrence of the three methods. The bars indicate R_n estimates at a common location within the field, that is, at the location of the Bowen-ratio apparatus as pictured in Figure 3. On the three days, the value of R_n estimated from TM data and that estimated using the Bowen-ratio radiometer differed by 8%, 5%, and -10% of the TM-based estimate, respectively. It differed from the aircraft-based estimates by 2%, -8%, and 12% on the three days.

Similar data for λE values are presented in Figures 5 and 6. Again, there was good correlation between the remote estimates and the Bowen-ratio estimates. Estimates of λE using TM data differed from Bowen-ratio estimates by 1%, -3%, and -3% on the three days, respectively. The difference between aircraft-based estimates and TM-based estimates were 5%, 9%, and 1%.

The data presented in Figures 3 and 5 illustrate the advantage of each method for evaluating energy balance. The Bowen-ratio technique provides continuous data over time but values are, for the most part, applicable only to a uniform area surrounding the instrument. The aircraft-based sensors provide data at intervals along a transect, but only at an instant in time. The satellite-based sensors are also limited to one-time-of-day measurements, but the data are spatially continuous.

CONCLUDING REMARKS

The results reported here indicate that a satellite-based technique will yield values of instantaneous λE and R_n from full-cover cropped fields that compare well with values measured with a Bowen-ratio method and an aircraft-based method. The major advantage of the satellite-based technique is the ability to produce local maps of λE and R_n. However, there are several aspects of the method that need further attention before it can be applied on an operational basis.

The reliable evaluation of sensible heat flux density using Eq. (6) is based on the assumption that T_s is the aerodynamic temperature, that is, the average temperature of all the canopy elements weighted by the relative contribution of each element to the overall aerodynamic conductance (McNaughton, 1988). The temperature measured by the thermal radiometer is the radiometric temperature, defined operationally as the temperature of the surface features exposed to the radiometer. Huband and Monteith (1986) stated that the aerodynamic and radiometric temperatures may not be the same for a crop canopy. Choudhury et al. (1986) found that the two temperatures were nearly the same for near-neutral conditions, but radiometric temperatures were higher than aerodynamic temperatures for stable conditions and lower for unstable conditions. McNaughton (1988) concluded that an error in T_s of 1°C would lead to a typical error of 50 W m^{-2} in H from crops and so to an equal error in λE.

This problem is compounded in the case of partial-cover crop canopies where T_s is actually a composite of the temperature of the plants, soil, and shaded surfaces. This results in measurements of surface temperatures that are dominated by the soil surface rather than by the transpiring vegetation. Thus, for the partial canopy case, H is commonly overestimated and values of λE based on Eq. (1) are underestimated. This problem has been explored by Kustas et al. (1987) over rangeland vegetation in the Owens Valley, California. It remains an active research topic.

A second issue, also related to evaluation of H, is the accurate estimate of surface roughness (z_0) and displacement height (d). These parameters are commonly estimated as a function of plant height (h). Over diverse agricultural regions, plant height is rarely known and cannot be estimated easily from satellite-based spectral data. However, there is some evidence that the nondimensional ratios z_0/h and d/h are related to plant density (Shaw and Pereira, 1982), a parameter than can be estimated from remote spectral data. These findings, based on a numerical model, raise the possibility of making rough estimates of both z_0 and d from satellite-based spectral data.

Correction of satellite-based spectral data for atmospheric effects is presently based on a concurrent set of measurements of atmospheric optical depth and surface temperature. This procedure is obviously inconvenient if the method were to be used on an operational basis. Ideally, a correction technique would be based on information that is readily available from conventional weather stations or from the satellite data itself. In any case, the correction procedure needs to be simplified in order to be incorporated into a convenient operational procedure.

Finally, there are difficulties in extrapolating ground-based measurements of air temperature (T_a) and wind speed (U) over complex terrain. Both T_a and U are sensitive to local topography and changes in surface cover. For example, Brown[2] reported differences in T_a of 5°C between instruments located in irrigated agricultural fields and adjacent desert land. Such measurement variation in T_a and U must be accounted for because it causes proportional variation in H [Eq. (6)]. A 5°C error in T_a could result in an error in H of 250 Wm^{-2}, thus accounting for the extraordinarily high values of H obtained from the region surrounding MAC (Fig. 2). To date, the remote method has been applied only to flat, uniform fields; the full potential of this method will not be realized, however, until the difficulties of more complex terrain are resolved.

[2]Personal communication, Paul W. Brown, Extension Biometeorologist, Dept. of Soil and Water Science, University of Arizona, Tucson, AZ 85721.

The work described in this paper was partly supported by NASA Grant No. 1967-IRP-38. The authors wish to acknowledge the excellent support and cooperation of the Maricopa Agricultural Center personnel.

REFERENCES

Brutsaert, W. H. (1975), On a derivable formula for long-wave radiation from clear skies, *Water Resour. Res.* 11:742–744.

Carlson, T. N., and Boland, F. E. (1978) Analysis of urban-rural canopy using a surface heat flux/temperature model, *J. Appl. Meteorol.* 17:998–1013.

Carlson, T. N., Dodd, J. K., Benjamin, S. G., and Cooper, J. N. (1981) Satellite estimation of the surface energy balance, moisture availability and thermal inertia, *J. Appl. Meteorol.* 20:67–87.

Choudhury, B. J., Reginato, R. J., and Idso, S. B. (1986), An analysis of infrared temperature observations over wheat and calculation of latent heat flux, *Agric. For. Meteorol.* 37:75–88.

Dejace, J., Megier, J., Kohl, M., Maracci, G. Reiniger, P., Tassone, G., and Huygen, J. (1979), Mapping thermal inertia, soil moisture and evaporation from aircraft day and night thermal data, in *Proc. of 13th Int. Symp. on Remote Sens. of Environ., Environmental Research Institute of Michigan, Ann Arbor, MI*, pp. 1015–1024.

Fuchs, M., and Tanner, C. B. (1966), Infrared thermometry of vegetation, *Agron. J.* 58:597–601.

Gay, L. W., and Greenberg, R. J. (1985), The AZET battery-powered Bowen-ratio system, in *Proc. of the 17th Conf. on Agric. and Forest Meteorol., Scottsdale AZ*, Am. Meteorol. Soc., Boston, MA, 181 pp.

Gurney, R. J., and Hall, D. K. (1983), Satellite-derived surface energy balance estimates in the alaskan sub-arctic, *J. Climate Appl. Meteorol.* 22:115–125.

Holm, R. G., Moran, M. S., Jackson, R. D., Slater, P. N., Yuan, B., and Biggar, S. F. (1989), Surface reflectance factor retrieval from Thematic Mapper data, *Remote Sens. Environ.* 27:47–57.

Huband, N. D. S., and Monteith, J. L. (1986), Radiative surface temperature and energy balance of a wheat canopy I: comparison of radiative and aerodynamic canopy temperature, *Boundary-Layer Meteorol.* 36:1–17.

Jackson, R. D. (1984), Total reflected solar radiation calculated from multiband sensor data, *Agric. Forest Meteorol.* 33:163–174.

Jackson, R. D. (1985), Evaluating evapotranspiration at local and regional scales, *Proc. IEEE* 73:1086–1096.

Jackson, R. D. (1988), Surface temperature and the surface energy balance, in *Flow and Transport in the Natural Environment: Advances and Applications* (W. L. Steffen and O. T. Denmead, Eds.), Springer-Verlag Berlin, Heidelberg, pp. 133–153.

Jackson, R. D., Hatfield, J. L., Reginato, R. J., Idso, S. B., and Pinter, P. J., Jr. (1983), Estimation of daily evapotranspiration from one time-of-day measurements, *Agric. Water Mgt.* 7:351–362.

Jackson, R. D., Pinter, P. J., Jr., and Reginato, R. J. (1985), Net radiation calculated from remote multispectral and ground station meteorological data, *Agric. Forest Meteorol.* 35:153–164.

Jackson, R. D., Moran, M. S., Gay L. W., and Raymond, L. H. (1987), Evaluating evaporation from field crops using airborne radiometry and ground-based meteorological data, *Irrig. Sci.* 8:81–90.

Kustas, W. P., Choudhury, B. J., Moran, M. S., Reginato, R. J., Jackson, R. D., and Gay, L. W. (1987), Use of surface temperature estimated from thermal infrared data to determine evapotranspiration over sparse canopy, in *18th Conf. on Agric. and Forest Meteorol.*, pp. 88–90.

Mahrt, L., and Ek, M. (1984), The influence of atmospheric stability on potential evaporation, *J. Climate Appl. Meteorol.* 23:222–234.

McNaughton, K. G. (1988), Surface temperature and the surface energy balance—commentary, in *Flow and Transport in the Natural Environment: Advances and Applications* (W. L. Steffen and O. T. Denmead, Eds.), Springer-Verlag, Berlin, Heidelberg, pp. 154–159.

Monteith, J. L. (1973), *Principles of Environmental Physics*, Arnold, London, 241 pp.

Moran, M. S. (1990), A window-based technique for combining Landsat TM thermal data with high-resolution multispectral data over agricultural lands, *Photogramm. Eng. Remote Sens.*, in press.

Price, J. C. (1980), The potential of remotely sensed thermal infrared data to infer surface soil moisture and evaporation, *Water Resour. Res.* 16:787–795.

Price, J. C. (1982), Estimation of regional scale evapotranspiration through analysis of satellite thermal-infrared data, *IEEE Trans. Geosci. Remote Sens.* 20:286–292.

Reginato, R. J., Jackson, R. D., and Pinter, P. J., Jr. (1985), Evaporation calculated from remote multispectral and ground station meteorological data, *Remote Sens. Environ.* 18:75–89.

Rosema, A., Bijleveld, J. H., Reiniger, P., Tassone, G., Blyth, K., and Gurney, R. J. (1978), TELL-US, a combined surface temperature, soil moisture and evaporation mapping approach, in *Proc. of the 12th Int. Symp on Remote Sens. of Environ.*, Environmental Research Institute of Michigan, Ann Arbor, MI, pp. 2267–2276.

Shaw, R. H., and Pereira, A. R. (1982), Aerodynamic roughness of a plant canopy: a numerical experiment, *Agric. Meteorol.* 26:51–65.

Slater, P. N., Biggar, S. F., Holm, R. G., Jackson, R. D., Mao, Y., Moran, M. S., Palmer, J. M., and Yuan, B. (1987), Reflectance- and radiance-based methods for the in-flight absolute calibration of multispectral sensors, *Remote Sens. Environ.* 22:11–37.

Soer, G. J. R. (1980), Estimation of regional evapotranspiration and soil moisture conditions using remotely sensed crop surface temperatures, *Remote Sens. Environ.* 9:27–45.

Spittlehouse, D. L., and Black, T. A. (1980), Evaluation of the Bowen ratio/energy balance method for determining forest evapotranspiration, *Atmosphere-Ocean* 18:98–116.

Taconet, O., Bernard, R., and Vidal-Madjar, D. (1986), Evapotranspiration over an agricultural region using a surface flux/temperature model based on NOAA-AVHRR data, *J. Climate Appl. Meteorol.* 25:284–307.

Taylor. S. E. (1979), Measured emissivity of soils in the southeast United States, *Remote Sens. Environ.* 8:359–364.